

Reliability Behavior of Surface Mount Devices Assembled with Bismuth Bearing Low-Melt Solder Pastes



Luke Wentlent, Michael Meilunas and Jim Wilcox

Abstract As the electronics industry continues to evolve in complexity, a concerted effort has developed to implement lower melting point solders. While several exist, one of the most popular has been the SnBi eutectic alloy. Although the process procedures required to create such assemblies is straight-forward, the reliability performance of the bismuth bearing alloys is not well documented and requires significant study before the materials can be adopted by the industry. This concern is compounded by the fact that the microstructural characteristics of the bismuth-based alloys are highly dependent upon processing parameters such as time and temperature when assembled in a “mixed” alloy system (i.e. combined with Tin-Silver-Copper) and it is theorized that such microstructural variability may result in significant thermo-mechanical reliability variations. Accordingly, BGA and LGA components were assembled using SnBi paste and subjected to thermo-mechanical cycling. Upon failure, the package reliability and interconnect failure mechanisms were studied.

Keywords Low-melt solder · Pb-free · Thermal cycling · BiSn

Introduction

As a consequence of the further advancement and innovation of the electronics industry, greater demands are being placed upon the materials involved in SMT assemblies. One critical aspect of this is the increasing desire to utilize solder alloys with a melting point lower than that of the conventional SnAgCu (SAC) system [1, 2]. Lower temperature reflow processes would enable different materials to be integrated, greater flexibility with regards to the assembly process (i.e. strategically attaching components with different melting point solders), and improving reliability by minimizing the warpage that an assembly will experience during reflow.

L. Wentlent (✉) · M. Meilunas · J. Wilcox
Universal Instruments Corp., 33 Broome Corporate Pkwy., Conklin, NY 13748, USA
e-mail: luke.wentlent@uic.com

© The Minerals, Metals & Materials Society 2020
The Minerals, Metals & Materials Society (ed.), *TMS 2020 149th Annual Meeting & Exhibition Supplemental Proceedings*, The Minerals, Metals & Materials Series, https://doi.org/10.1007/978-3-030-36296-6_67

While a variety of solder alloys exist with lower melting points than that of the SAC system, the BiSn-eutectic or near-eutectic BiSn1.0Ag systems are currently the most popular. These alloys are available as either a paste or preform and possess a melting point of 139 °C [3, 4]. These systems are not particularly novel, as the BiSn system was once considered a candidate to replace SnPb early in the transition to the Pb-free standard. However, if contaminated with Pb, the BiSn system can produce a eutectic phase with a melting point of 96 °C [5]. Due to this, among other more mechanical reliability concerns, BiSn solders were set aside for the more promising SAC system. Despite this, BiSn solders continued to attract interest due to their low melting point and research upon them persisted. This proved advantageous as with Pb completely phased out of the majority of the electronics industry, the concerns of Pb contamination are virtually nonexistent. Accordingly, there has been renewed interest in integrating low melting point BiSn solders in electronics assembly.

Over the past 10 years, a range of studies has investigated the wettability, creep behavior, interfacial reactions, and electromigration reliability of the binary BiSn system [6–12]. These studies have shown that the high quantities of Bi present make the system relatively unstable and prone to reliability concerns regarding a loss of ductility. Two specific issues are the loss of ductility due to Bi embrittlement of the Cu₆Sn₅ intermetallic compound (IMC) layer and a decrease in reliability due to Bi segregation at the IMC-solder interface [13–15]. While undesirable from a reliability perspective, this loss of ductility has clear implications for high-strain rate environments (i.e. drop testing or high-speed shear). Accordingly, further investigations by the authors have studied the sensitivity of BiSn interconnects to the strain rate [16]. It was shown that after certain processing conditions, the Bi within the system will drive a sharp transition in failure and fracture modes accompanied by a drop in shear strength. This is attributed to a combination of Bi-rich phases being highly incoherent with respect to the Sn matrix, Bi-rich phases accumulating in large quantities along the IMC layer, and Bi acting to embrittle the intermetallic compounds [17, 18].

An additional complication is the unfortunate near-term reality of integrating this alloy into the industry on a large scale. As the demand has not existed until this point in time, most electronic components will not be easily available with BiSn preforms. Therefore, the most common approach to utilizing BiSn solder is to print the BiSn paste and place a package balled with a SAC solder on top of it. This assembly would then be reflowed at a lower temperature appropriate for the low melting point paste (i.e. below 217 °C). On the surface, these joints may appear much like any typical interconnect; however, joint microstructures will lack the homogeneity of pure SnAgCu solders. Instead, the resulting interconnect will be a mixed BiSn-SAC solder joint, containing two distinct regions; one consisting primarily of SnAgCu and one consisting of BiSn. The reason for the distinct microstructural phases is that the degree of mixing between the SAC solder bump and the BiSn solder paste is highly dependent upon the paste metal to solder bump metal volume fraction, time about 139 °C, and peak processing time/temperature. Improved mixing is expected as paste volume increases relative to the solder bump volume as there is more molten BiSn to locally interact with the solder bump. Increasing the time above 139 °C also improves

mixing as the additional time allows for continued localized melting. Peak processing temperature may be the largest factor affecting the solder alloy mixing with faster-localized interactions and accelerated diffusion rates expected as the temperature rises. It is not unreasonable to postulate that this heterogeneous microstructure will result in non-trivial variations in mechanical behavior and thermo-mechanical reliability. Indeed recent studies investing these “mixed” or “hybrid” solder joints have shown significant variability based upon process parameters and a constantly evolving microstructure due to the poor stability of the Biphase regions [7, 10, 13].

Although the basic behavior of the solder joint microstructure of mixed SnAgCu+BiSn systems is understood, the reliability of such solder joints remains uncertain. The experiment described in this report begins to address this concern by evaluating for BGA (mixed SAC-BiSn) and LGA (pure BiSn) assemblies using accelerated thermal cycling. Five assembly conditions were created with various peak reflow temperatures of 150, 175, or 200 °C and time above 139 °C ranging from 60 to 160 s. The failure mechanisms and behaviors of select samples were studied via optical and scanning electron microscopy and inferences made as to performance in-service conditions.

Experimental

The test vehicles utilized for the experiment were created using a custom-designed test board and-chained components purchased from Practical Components. The board was acquired with a copper OSP surface finish and measured approximately 190 × 140 mm and was approximately 2.5 mm thick.

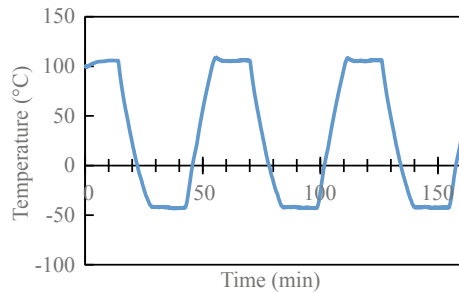
The test vehicle was designed to house two replicates each of nine surface mount devices: CABGA256, MLF100, DRMLF156, BGA144, CABGA208 (LGA formats were also used), CVBGA97, PBGA676, and BGA360. The CABGA256, CABGA208, and CALGA208 performance and behaviors will be the topics of interest in this document. All nine of the device designs were either bumped with SAC 305 eutectic solder or supplied with matte tin or a gold over nickel finish. The devices were stitched patterned dummy components and the mating stitch pattern was included on the test board in order to form a complete daisy-chain circuit for monitoring second level solder joint interconnections.

The test vehicles were assembled using a solder paste printing process. Four of the sample legs utilized a near-eutectic BiSn1.0Ag solder composition while one additional test cell used the more conventional eutectic BiSn, see Table 1.

Four reflow profiles were created for the experiment. All four profiles were direct ramp type and were created for a BTU Pyramx 125N forced convection oven containing a nitrogen atmosphere. The profiles produced different peak solder joint temperatures and/or time above 139 °C. The three peak reflow temperatures examined were 150, 175 and 200 °C. The time above 139 °C was kept constant at 60 s except for one 175 °C leg where it was increased to 160 s, see Table 1. Cycling was performed in a Thermotron model F82 chamber. The samples were subjected to a

Table 1 Description of the different experimental legs in this study

		Quantity tested		
Reflow profile	Paste	BGA256	BGA208	LGA208
(A) 150 °C, 60 s	BiSnAg	16	16	16
(B) 175 °C, 60 s	BiSnAg	16	16	16
(C) 175 °C, 60 s	BiSn	16	16	–
(D) 175 °C, 160 s	BiSnAg	16	16	–
(E) 200 °C, 60 s	BiSnAg	16	16	16

Fig. 1 Graph showing the accelerate thermal cycling test temperature cycling

56 min, -40 to 105 °C environment with 15 min dwell periods as the temperature extremes and 11 °C per minute transition rates, see Fig. 1. Samples were monitored in situ and removed from the thermal chamber on a weekly basis.

Thermal cycling was performed for a period of five months, resulting in a total of 4200 cycles. A Weibull lifetime analysis was performed for each test population with 44% or greater failure occurrence. Samples removed for failure analysis were mounted in epoxy and mechanically cross-sectioned for further analysis. The failure mechanisms and modes were characterized using a combination of optical microscopy (OM), scanning electron microscopy (SEM), and energy dispersive X-ray analysis (EDX).

Results and Discussion

As Reflowed Microstructure

Initial observations of the microstructure after reflow showed a similar morphology for the two BGA packages, see Fig. 2. The top of the mixed joint appears to be composed primarily of the original SAC solder bump while the bottom region is the BiSn(Ag) paste deposit. In all of the samples reflowed at 150 or 175 °C the microstructure was highly stratified with a relatively clear delineation between the two regions. This demarcation line appears to be representative of a transition point

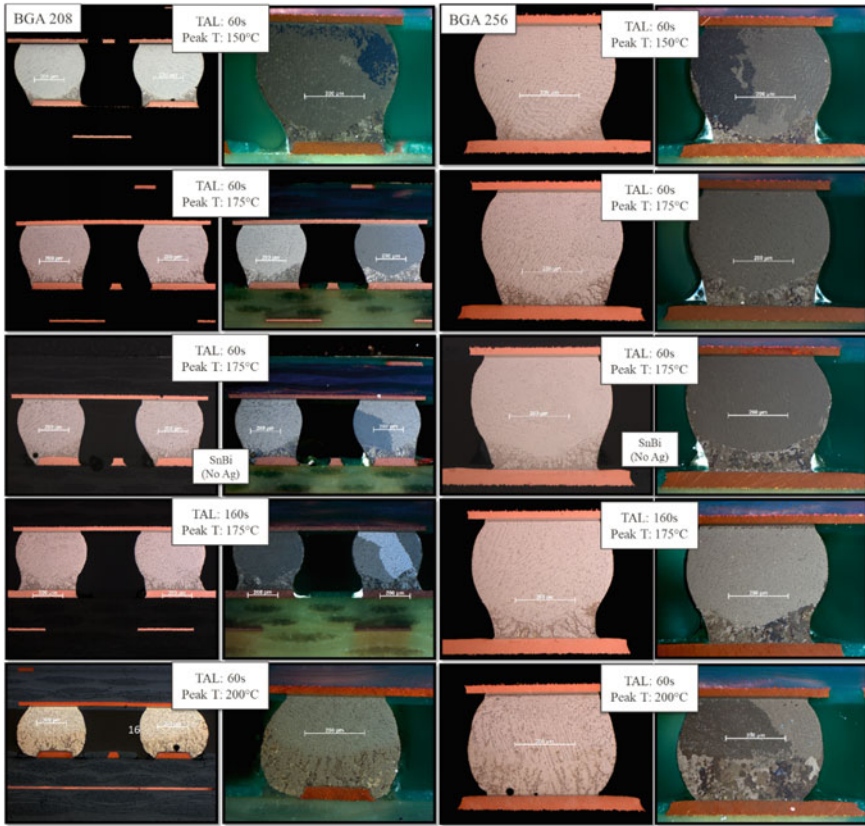


Fig. 2 Bright field photographs of the BGA 208 and BGA 256 packages after reflow. Note the similarity of the microstructure for the different reflow profiles, with the exception of the samples reflowed with a peak temperature of 200 °C

in the Bi concentration. Above this line, no Bi-phases are present indicating that all of the Bi must be in solid solution (solubility of Bi in Sn ~6 wt% at room temperature [3]) while below this transition zone it is quite clear that a large quantity of Bi precipitates is present. In contrast, when the temperature was increased to 200 °C the size of the zone containing Bi precipitates increased substantially. In the majority of the samples examined the abrupt transition point between the two zones was, while still present, no longer as prominent. Prominent Bi-rich phases were present throughout the entire bottom half of the interconnect, representing a substantial increase in the degree of mixing that occurred. Comparing the two sample legs reflowed at 175 °C with different times above 139 °C (60 and 160 s), no obvious differences in the microstructure were visible. In both sample sets the degree to which the interconnect had mixed were relatively similar. It would seem that rather than time above liquidus it is the peak reflow temperature which will drive the degree of mixing.

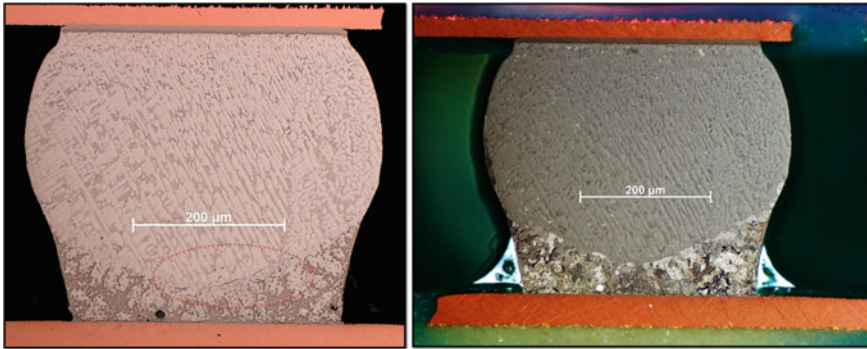


Fig. 3 Bright field and cross-polarized image of a BGA 208 as-reflowed cross-section. Note the prominent grain boundaries that are visible along the transition zone

Cross-polarized investigations showed a markedly different microstructure than typically observed in SAC 305 solder joints. The upper zone of the joint, that did not appear to melt during reflow, was a typical single crystal or “beach ball”, while the lower region of the interconnect appeared to be polycrystalline. The nature of this crystallographic morphology is likely due to a combination of the solidification kinetics at the lower peak temperatures and numerous nucleation points that are present. It appears that the demarcation line between the SAC bump and BiSn paste is also the location of a relatively energetic boundary. In a number of cross-sections, specific β -Sn grains were observed slightly extruding out of the section surface, see Fig. 3. This is a phenomena often observed in recrystallized SAC samples where, given time, recrystallized grains will slightly extrude out of the sample surface in an effort to relieve the energy inherent to a misoriented grain and its boundaries.

Examination of the LGA 208 samples showed a solder interconnect where the Bismuth precipitates were evenly distributed throughout the joint. Examination via cross-polarized microscopy appears to show the presence of a multi-granular structure. That said, it does not appear to be as prominent as that observed in the BiSn paste region of the mixed assemblies. In the BGA 208 and 256 samples, the Bi appeared to have precipitated in a somewhat vertical alignment. This morphology was not observed with the LGA 208 samples; instead, the Bi possessed a much more random patterning (Fig. 4).

ATC Failure Behaviors

Upon failure in thermal cycling, select samples were removed and cross-sectioned so as to ascertain the failure mechanisms. Both BGA packages displayed similar mechanisms, with failure occurring via a crack propagating through the lower BiSn region of the solder joints. The samples reflowed at 150 and 175 °C showed a large

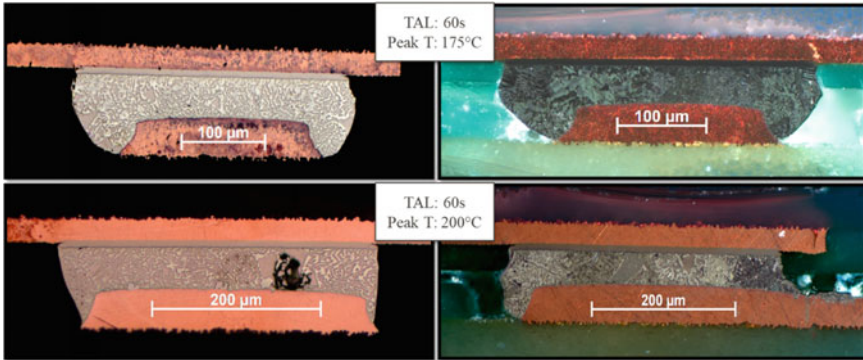


Fig. 4 Bright field and cross-polarized images of the LGA 208 package after reflow

amount of separation of the solder from the Cu_6Sn_5 IMC layer. In some cases, it appeared that the failure began to shift up into the solder slightly with the failure crack traveling through the solder along phase boundaries. Packages reflowed at 200 °C showed no signs of cracking within the BiSn region; rather, a hairline fracture was visible along the aforementioned boundary marking the transition between the BiSn region and remaining SAC bump, see Figs. 5, 6, and 7.

The generally accepted failure process in SnAgCu solder joints is one of precipitate coarsening followed by recrystallization and eventual cracking along the recrystallized grain boundaries. It appears that a fundamentally different failure process is occurring in the mixed solder joints. First, while the lower region of the failed solder joints possesses a polycrystalline grain structure, it is unlikely that these are recrystallized grains. Rather, it is more probable that these are coarsened grains from the initial as-reflowed condition. Higher magnification images show that the crack propagated through the joint by traveling along with a combination of grain boundaries and phase boundaries between the Bi precipitates and the β -Sn matrix. It has been reported that Bi precipitates in the Sn matrix are relatively incoherent [17] so it is not unexpected that these boundaries provide a preferential crack propagation pathway, see Fig. 6. In some cases it appears that the crack actually split through a Bi precipitate, not unsurprising given the known brittle nature of Bismuth.

It does appear that if enough mixing can occur then the relatively lower number density of Bi precipitates within the bottom of the joint will, in turn, allow the crack to propagate along the existing grain boundaries. This was observed in the BGA samples reflowed with a peak temperature of 200 °C. In both cases, the majority of the failures occurred via a separation of the upper and lower regions of the solder joint, see Fig. 7. It appears that this boundary is energetic enough to provide a prime location for failure. The difference in failure mechanisms between the 175 and 200 °C samples indicates that there is a significant impact of the processing parameters on the reliability of the interconnect, perhaps more so than typically seen with conventional SAC solders.

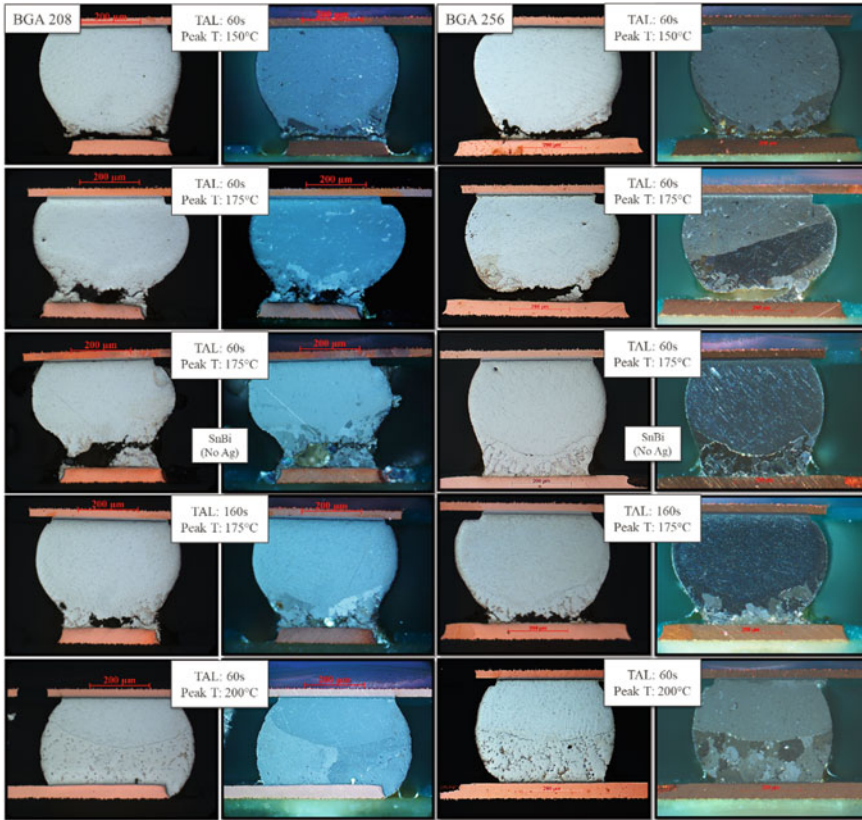


Fig. 5 Bright field and cross-polarized photographs of BGA 208 and BGA 256 samples after failure in accelerated thermal cycling

Interestingly, opposing trends were observed when the failure distributions were examined. As Fig. 8 shows, the samples reflowed with a peak temperature of 200 °C were the top performers while those reflowed with a peak temperature of 150 °C were the worst. A completely opposite trend was observed when looking at the performance of the BGA 256 package. In this case, the samples reflowed with a peak temperature of 200 °C was the worst performer and 150 °C the best. There is no clear explanation for this based upon the microstructure at this point in time; however, it should serve to highlight the variability that has become associated with the use of Bismuth in the SAC system.

The LGA 208 samples showed a similar failure mechanism to that of the BGA samples reflowed at 150 and 175 °C. In all of the samples examined the crack appeared to propagate primarily along the boundaries between the Bi precipitates and the β -Sn matrix, see Fig. 9. Examination of the failure distributions, see Fig. 10, showed that the samples reflowed with a peak temperature of 200 °C were the peak performers. Interestingly, the performance between the LGA and BGA 208 was

Fig. 6 Bright field and cross-polarized images of a failed BGA 256 solder joint.
Note The path of the crack as it propagates through the solder joint

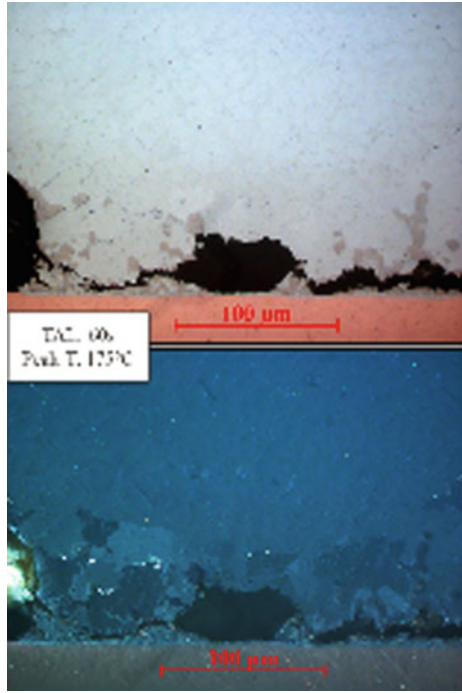
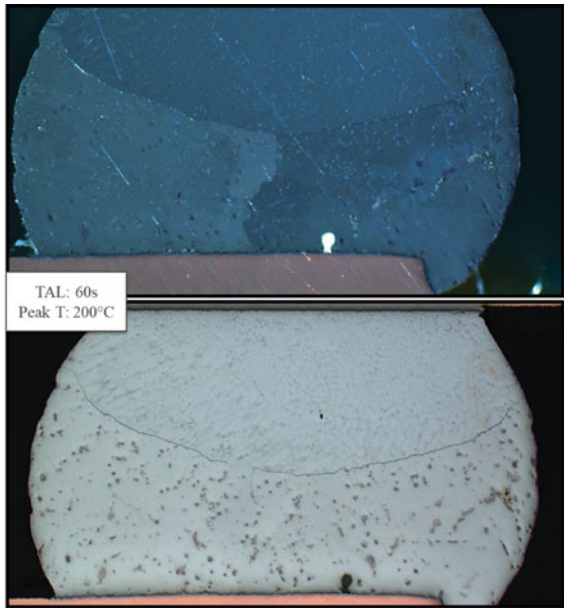


Fig. 7 Bright field and cross-polarized images of a BGA 256 solder joint after failure in thermal cycling.
Note The presence of the hairline fracture along the boundary of the two regions of the solder joint



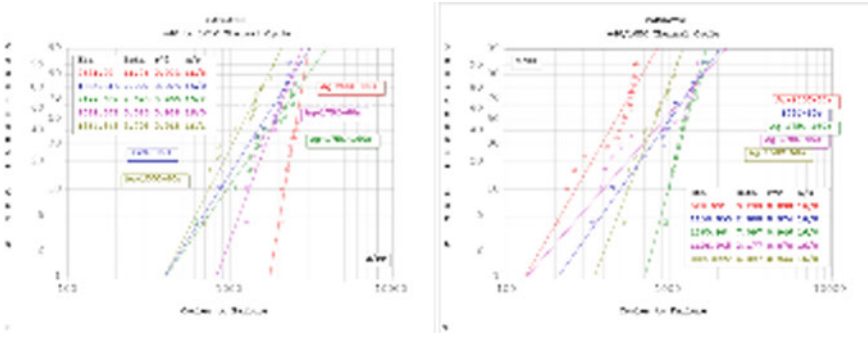


Fig. 8 Weibull Plots for BGA 208 and 256 components. *Note* The contrasting performance of the different experimental legs

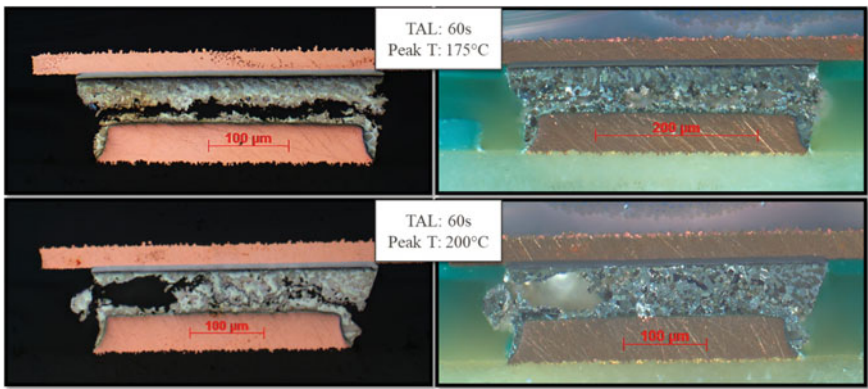


Fig. 9 Bright field and cross-polarized images of LGA 208 samples after failure in accelerated thermal cycling

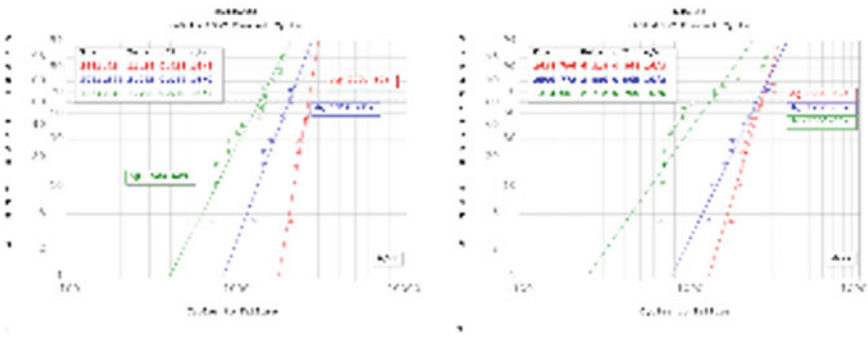


Fig. 10 Weibull plots showing the failure distributions of the BGA 208 and LGA 208 packages. *Note* The virtually identical performance for the two package types

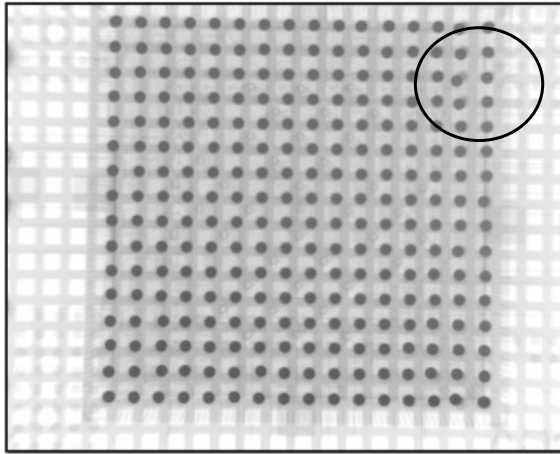


Fig. 11 X-ray of BGA 256 package reflowed with a peak temperature of 200 °C. Notice the solder joint out of alignment encircled in the image

almost identical for the three different sample legs compared. While intriguing at face value, this observation has important implications regarding the role of the SAC bump. In BGA 208 joints, the failures were almost always confined to the lower region of the joint where the Bi has precipitated out of the Sn matrix. Additionally, the failure mechanisms between the two package types was virtually identical, crack propagation along the phase and grain boundaries. What this indicates is that the SAC bump is playing little to no role in providing any boost or enhancement in reliability when comparing a SAC/BiSn mixed assembly BGA and a pure BiSn LGA.

Typically when samples are removed from thermal cycling, aside from probing to identify the failure chain they are examined via X-ray. Upon closer examination, it was noticed that in a handful of locations individual solder joints were located significantly out of position, see Figs. 11 and 12. This phenomena was observed for both BGA 208 and BGA 256 packages for all reflow conditions.

A select sample was identified and a cross-section prepared to allow observation of the row containing a clearly shifted joint, see Fig. 13. As the X-ray image in the figure shows, the third joint from the lower-left-hand corner of the package appears to be significantly shifted from its typical position. When examining that same joint in cross-section it is clearly located several hundred microns to the right. Closer examination of the sample showed that the lower BiSn region was significantly elongated while the top of the joint appeared to have shifted out over the solder mask. There is some recrystallization of the β -Sn grain present in the top of the joint but this is likely the byproduct of the interconnect being shifted to such a degree, as opposed to the driving force for this behavior. Investigation via SEM showed that it appears the top of the joint is tearing in a semi-tensile manner. As one of the images in Fig. 15 shows the solder has the appearance of a puzzle piece, where it is clear how it fits back together. EDX analysis of this upper region of the interconnect

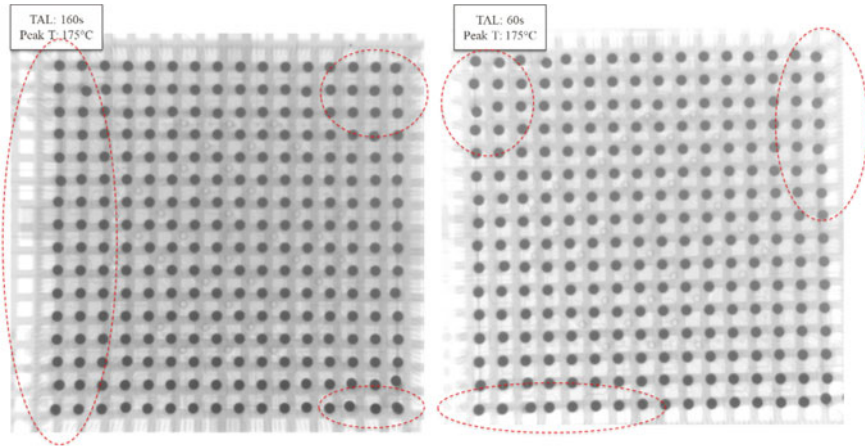


Fig. 12 X-ray images of BGA 256 packages after accelerated thermal cycling. Observe the numerous joints that are shifted out of position, outlined in red

where this crack is located showed only trace amounts of Bi to be present in solid solution (~ 1 wt%). Interestingly enough, despite this highly unusual behavior, the solder interconnect examined here was still electrically connected and was not the failure location for this sample. This was typically the case for the other instances of this “solder drift” phenomena observed in this study (Fig. 14).

A cross-section of a package was prepared by cross-sectioning in the vertical direction, see Fig. 16. This allowed observations of the top of the solder joints which appeared to show unique striations along the top of the joints that had shifted, see Fig. 17. It is suggested that these striations are indicative of some type of mechanism that is cyclic in nature, with some of the joint movement occurring as a function of the thermal cycle. Observations of more samples showed that the majority of the shifted interconnects were located in the perimeter rows of the package. Additionally, the direction that they had shifted all appeared to be loosely radial in nature. This would indicate that there is some dependency upon the distance to neutral point as well. Regardless of the mechanism, this joint shifting was observed in almost every failed package examined and merits further study.

Conclusion

The performance of BiSn(Ag) assemblies in accelerated thermal cycle testing was examined and the failure mechanisms identified. As shown in Fig. 2 there is clearly a unique as-reflowed microstructure for the mixed SAC-BiSn(Ag) assemblies. The microstructure is highly heterogeneous consisting of a relatively conventional SnAgCu microstructure in the upper half and a lower region where a significant

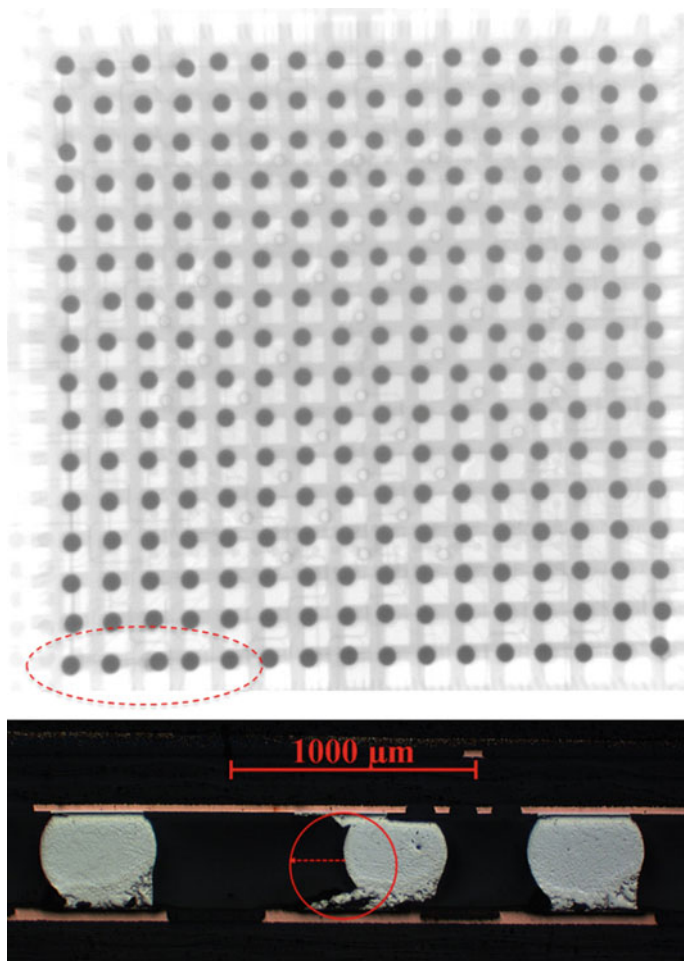


Fig. 13 X-ray image and accompanying cross-section showing the shifted joint

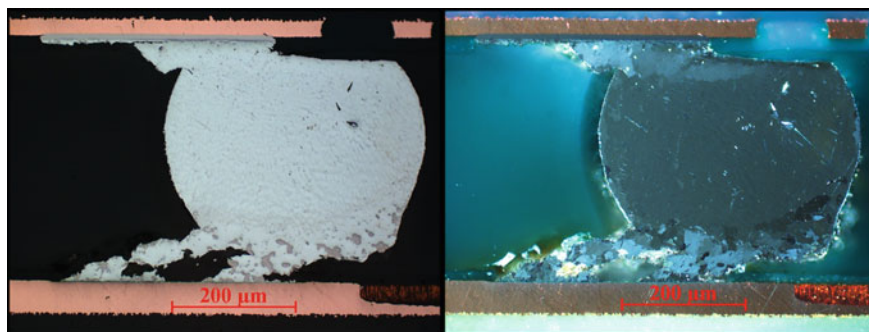


Fig. 14 Bright field and cross-polarized image of a BGA256 sample

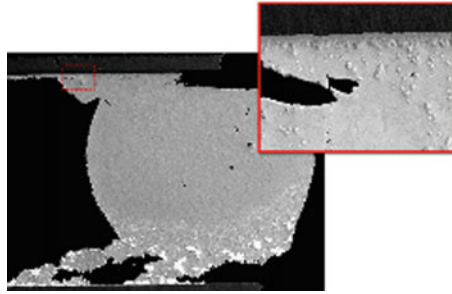


Fig. 15 SEM images of the joint from Figs. 13 and 14. *Note* How the torn pieces of the solder appear to fit together like puzzle pieces

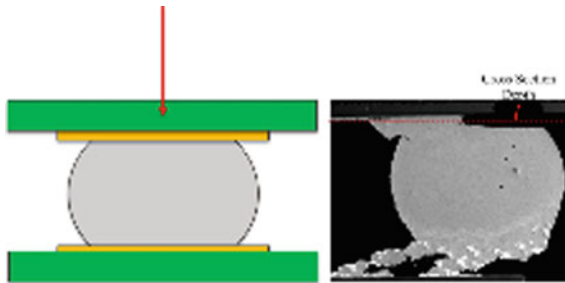


Fig. 16 Image explaining the cross-section direction to examine the top of the solder joint

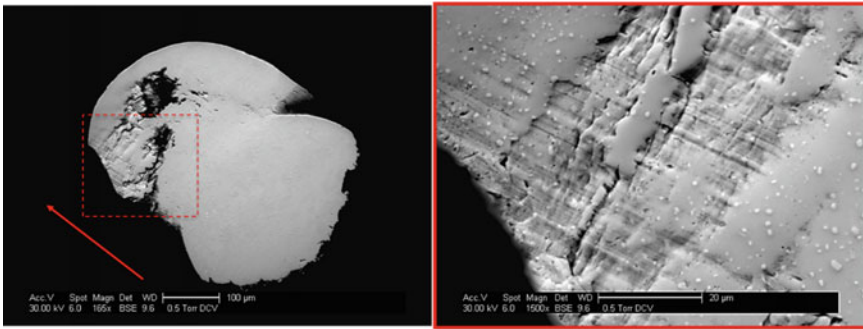


Fig. 17 Vertical cross-section of a mixed joint that appeared to have shifted during thermal cycling

amount of Bi precipitated out of the solution. This lower region is polycrystalline in nature and has a fairly well-defined boundary with the upper SAC section. The LGA samples were all polycrystalline in nature and the Bismuth precipitates were evenly distributed throughout the joint.

The two BGA packages examined showed similar failure mechanisms in accelerated thermal cycling. In both cases, the 150 and 175 °C failures consisted of a crack propagating along the phase boundaries between the Bi and Sn or along the grain boundaries existing within the polycrystalline high Bi region. This was a similar mechanism as what was observed in the LGA samples, where the crack also clearly propagated along the phase boundaries. The samples reflowed with a peak temperature of 200 °C showed a slightly different mechanism where failure appeared to occur via separation of the upper and lower regions of the interconnect. The failure distributions for the BGA 208 and BGA 256 showed that there was a completely different performance of the different reflow profiles. For example, the samples reflowed with a peak temperature of 200 °C were the top performers for one package type but the worst for the other. No explanation for this was obvious when the microstructure was examined so further work is necessary. The performance of the BGA 208 and LGA 208 packages was almost identical when the failure statistics were examined. This close performance, as well as the similar failure mechanism, would seem to indicate that the additional solder volume gained from the SAC bump is imparting no additional increase in performance. In other terms, a mixed SAC-BiSn(Ag) BGA package would perform identically to a BiSn(Ag) LGA package.

Finally, a unique phenomenon was observed where in a number of instances the mixed interconnect would appear to have drifted or shifted out of its typical position after thermal cycling. This behavior was observed with both BGA package types and for all of the reflow profiles examined. Closer examination of interconnects that had shifted only gave a partial explanation for this unique behavior. It appears that it is related, at least in part, to the joint position in the solder joint array. All of the shifted joints were located in the out rows on the package. Additionally, it appears that this shift is cyclic in nature, occurring dynamically in small increments throughout the entire thermal cycling.

References

1. Ribas M, Chegudi S, Kumar A, Pandher R, Raut R, Mukherjee S et al (2013) Development of low-temperature drop shock resistant solder alloys for handheld devices. In: IEEE 15th electronics packaging technology conference, Singapore
2. Fu H, Aspandiar R, Chen J, Cheng S, Chen Q, Coyle R et al (2017) iNEMI project on process development of BiSn-based low temperature solder pastes. In: SMTA international conference and exhibition, Rosemont, Illinois
3. Belyakov S, Gourlay C (2017) Recommended values for the B-Sn solidus line in Sn-Bi alloys. *Thermochimica Acta* 654:65–69
4. Vianco P, Rejent J (1999) Properties of ternary Sn-Ag-Bi solder alloys: part I—thermal properties and microstructural analysis. *J Electron Mater* 28:1127–1137
5. Felton L, Raeder C, Knorr D (1993) The properties of tin-bismuth alloy solders. *J Minerals Metals Mater Soc* 45(7):28–32
6. Li Y, Chan Y (2015) Effect of silver (Ag) nanoparticle size on the microstructure and mechanical properties of Sn58Bi-Ag composite solders. *J Alloy Compd* 645:566–576
7. Liu Y, Sun F, Liu Y, Li X (2014) Effect of Ni, Bi concentration on the microstructure and shear behavior of low-Ag SAC-Bi-Ni/Cu solder joints. *J Mater Sci Mater Electron* 25:2627–2633

8. Osorio W, Peixoto L, Garcia L, Mangelinck-Noel N, Garcia A (2013) Microstructure and mechanical properties of Sn-Bi, Sn-Ag, and Sn-Zn lead-free solder alloys. *J Alloys Compd* 572:97–106
9. Zhao J, Qi L, Wang X, Wang L (2004) Influence of Bi on the microstructures evolution and mechanical properties in Sn-Ag-Cu lead-free solder. *J Alloys Compd* 375:96–201
10. Wang F, Huang Y, Du C (2016) Mechanical properties of SnBi-SnAgCu composition mixed solder joints using bending test. *Mater Sci Eng A* 668:224–233
11. Belyakov S, Xian J, Sweatman K, Nishimura T, Akaiwa T, Gourlay C (2016) Influence of bismuth on the solidification of Sn-0.7Cu-0.05Ni-xBi/Cu joints. *J Alloy Compd* 701:321–334
12. Shen L, Lu P, Wang S, Chen Z (2013) Creep behaviour of eutectic SnBi alloy and its constituent phases using nanoindentation technique. *J Alloy Compd* 574:98–103
13. Chen O, Molina A, Aspandiar R, Byrd K, Mokler S, Tang K (2015) Mechanical shock and drop reliability evaluation of the BGA solder joint stack-ups formed by reflow soldering SAC solder balls BGAs with BiSnAg and resin reinforced BiSn-based solder pastes. In: SMTA international conference and exhibition, Rosemont, Illinois
14. Liu P, Shang J (2001) Interfacial embrittlement by bismuth segregation in copper/tin-bismuth Pb-free solder interconnect. *J Mater Res* 16(6):1651–1659
15. Zhao J, Qi L, Wang L (2006) Effect of Bi on the kinetics of intermetallics growth in Sn-3Ag-0.5Cu/Cu solder joint. In: Proceedings of HDP
16. Wentlent L (2018) SnBi-SnAgCu mixed assemblies: microstructure and strain rate sensitivity. AREA Consortium, Binghamton
17. Belyakov S, Xian J, Zeng G, Sweatman K, Nishimura T, Akaiwa T, Gourlay C (2019) Precipitation and coarsening of bismuth plates in Sn-Ag-Cu-Bi and Sn-Cu-Ni-Bi solder joints. *J Mater Sci Mater Electron* 30:378–390
18. Delhaise A, Chen Z, Perovic D (2019) Solid-state diffusion of Bi in Sn: effects of B-Sn grain orientation. *J Electron Mater* 48(1):32–43